J Appl Electrochem (2008) 38:1599–1607
DOI 10.1007/s10800-008-9601-8

ORIGINAL PAPER

Impedance spectroscopy studies of the dissolution of ferrous- and zinc-based materials in aqueous timber preservatives

Gareth Kear · Hǎi-Zhèn Wú · Mark S. Jones · Frank C. Walsh

Received: 21 January 2008 / Accepted: 19 May 2008 / Published online: 4 June 2008

Abstract The relative degradation rates of metallic materials in aqueous, copper-based timber preservatives have been investigated using electrochemical impedance spectroscopy. The metals examined were AS/NZS 1595:1998, grade CA1 mild steel, AISI 316 stainless steel (UNS S31600) and AS 1397, grade Z275 hot-dipped galvanised coil-coated sheet. The electrolytes consisted of commercially sourced copper–chrome–arsenate, copper azole and alkaline copper quaternary electrolytes diluted to a concentration of 0.1 mol dm^{-3} copper. The electrochemical impedance response of each system has been modelled and the resulting relative rates of corrosion have been shown to broadly correspond to general trends taken from previous weight loss and direct current studies incorporating similar electrolytes. The hot-dipped galvanised steel corroded in an active manner at rates that were two to four orders of magnitude greater than that of the ferrous-based materials; the latter appeared to passivate in all instances.

Keywords Electrochemical impedance spectroscopy · Aqueous timber preservative · Corrosion · CCA · CuAz · ACQ · Hot-dipped galvanised steel · 316 stainless steel · Mild steel

1 Introduction

The tightening of health regulations describing the use of long established copper–chrome–arsenate (CCA) timber preservatives has taken place in most developed regions of the world [1–3]. Such changes have resulted in the widespread utilisation of relatively unproven copper-based alternatives such as copper azole- (CuAz) and alkaline copper quaternary- (ACQ) formulations [4–6]. Typically, these preservatives contain additives such as copper/tebuconazole or copper/didecylthyl ammonium chloride. Recent weight loss studies of materials in contact with timber have shown that these alternatives are considerably more corrosive towards mild steel and hot-dipped galvanised steel relative to CCA. This literature has been reviewed in detail elsewhere [7], where it is clear that there is growing concern related to adequate performance of CuAz and ACQ preservatives and an increasing commercial interest in the development of more suitable novel additives.

Both weight loss [8] and direct current derived corrosion rates [9] of zinc-based materials in aqueous timber preservatives have been shown to be orders of magnitude higher than that of mild steel and stainless steel (Table 1). Moreover, mild steel and 316 stainless steel passivate rapidly and effectively in the CCA, CuAz and ACQ electrolytes. Conversely, it is known that when the same materials are brought into contact with treated timbers, the degradation rates of galvanised steel, and particularly mild

G. Kear (✉) · H.-Z. Wú · M. S. Jones
Building Research Association of New Zealand (BRANZ) Ltd., Science and Engineering Services, Private Bag 50 908, Porirua 5240, New Zealand
e-mail: g.kear@soton.ac.uk

Present Address:
G. Kear
Electrochemical Engineering Laboratory, Energy Technology Research Group, School of Engineering Sciences, University of Southampton, Highfield, Southampton SO17 1BJ, UK

F. C. Walsh
Electrochemical Engineering Laboratory, Energy Technology Research Group, School of Engineering Sciences, University of Southampton, Highfield, Southampton SO17 1BJ, UK

steel are much higher in the CuAz and the ACQ wood than the equivalent CCA formulation [7, 10].

A simple correlation between metallic degradation rates measured in timber and 100% aqueous preservatives, therefore, appears to be difficult to achieve. Due to the perceived simplicity of practical measurements made in liquid electrolytes and a lack of effective technology transfer to the building industry, the analogy between corrosive media is still commonly utilised in product development and industry test standards [8, 11]. However, funding and technical support for investigations in both timber and liquid media is now being supplied by the affected regional building authorities, public sources and the fastener manufacturing industry.

The data produced using the AWPA E17 standard test [11], as shown in Table 1, were derived after exposure to comparatively elevated temperatures (300 ± 6 K), continuous electrolyte agitation and considerably lower concentrations of copper (0.02 mol dm^{-3} [CCA and ACQ] and 0.03 mol dm^{-3} [CuAz]). Moreover, the electrolytes used in the direct current measurements contained 0.3 mol dm^{-3} sodium sulfate (Na_2SO_4), although the environmental conditions and the dilution factor, with respect to copper, were identical to the current work. Previous voltammetry studies provided neither voltammetric curves that display true Tafel slopes nor linear behaviour at low values of polarisation relative to the corrosion potential (E_{corr}) [9]. In the majority of cases, therefore, absolute rates of corrosion could not be derived with complete confidence via direct current produced polarisation resistance used in conjunction with the Stern-Geary [12] relationship. Only a broad, qualitative analysis relating the state of materials passivation could be made.

The high solution resistance of the CuAz and ACQ aqueous preservatives also introduces limitations on accuracy when using direct current methods. For the electrolytes used in this work, for example, the values of electrolyte conductivity (concentrate as supplied) were CCA: 54.4 mS cm^{-1}, CuAz: 0.6 mS cm^{-1} and ACQ: 8.6 mS cm^{-1} [8, 9]. When diluted to 0.1 mol dm^{-3} copper, which is a typical value of preservative retention in timber [4], the equivalent values are 31.5, 4.8 and 6.4 mS cm^{-1}, respectively. The pH values of the preservatives in aqueous solution also vary significantly. The pH values for these diluted electrolytes are 1.3, 10.0 and 9.9, respectively.

Due to the complications resulting from a high solution resistance in high polarisation direct current techniques, electrochemical impedance spectroscopy (EIS) has been applied in this work to estimate the performance of mild steel, hot-dipped galvanised steel and AISI 316 stainless steel in the common, copper-based aqueous timber preservatives. The aim is to derive relative rates of materials degradation in liquid preservatives which can be used to verify the previous weight loss and direct current electrochemical investigations presented in Table 1. This is a novel approach for the corrosion testing of preservatives that are not in direct contact with timber fibres. An analogous application of EIS was made by Wojtowicz and Piwowarczyk [13] who used zinc-based materials in a slurries of timber fibre treated with phosphate derived timber additives (non-copper-based fire retardants). General inferences regarding the effectiveness of passivation

Table 1 AWPA E17 [11] derived standard weight loss corrosion rates [8] and active–passive behaviour [9] of ferrous- and zinc-based materials in diluted CCA, CuAz and ACQ electrolytes

	AWPA E17 corrosion rate/mm y^{-1}	Active–passive response[a]
CCA	0.02–0.03 mol dm^{-3} Cu	0.1 mol dm^{-3} Cu, 0.3 mol dm^{-3} Na_2SO_4
Mild steel	0.004 ± 0.001	Intermediate activity[b]
316 Stainless steel	(8 ± 6) × 10^{-5}	Passive
HDG	0.664 ± 0.081	Active
CuAz		
Mild steel	0.004 ± 0.001	Passive
316 Stainless steel	(28 ± 7) × 10^{-5}	Passive
HDG	0.009 ± 0.001	Intermediate activity[b]
ACQ		
Mild steel	0.004 ± 0.001	Passive
316 Stainless steel	(25 ± 8) × 10^{-5}	Passive
HDG	0.023 ± 0.003	Intermediate activity[b]

[a] The active–passive response was estimated from the results of direct current anodic voltammetry performed immediately after initial immersion of the electrode material. Details of active–passive criteria are given elsewhere [9]

[b] The material passivated rapidly after exposure (<2 h) as noted by polarisation resistance transient measurements [9]

were derived using impedance measurements with contribution from direct current measurements. However, the work is not directly applicable to this investigation as values of metallic degradation rate were not presented; neither were results for single-phase liquid electrolytes.

2 Experimental procedure

Triplicate experiments were performed at 294 ± 1 K over periods of 24 h. CCA-C (containing oxide species) concentrate and CuAz concentrate (CA-B) were supplied by Koppers Arch, New Zealand and ACQ-B concentrate was supplied by Osmose, New Zealand. The specified range of concentrate composition of each concentrate, as supplied by each manufacturer, is presented in Table 2. The concentrations of aqueous copper in each of the timber preservative concentrates were also determined independently using X-ray fluorescence. The timber preservative solutions were diluted with distilled water to give 0.1 mol dm^{-3} concentrations of copper. All electrolytes were examined in a fully aerated state through the application of gas diffusion with either air over a period of 10 min immediately before the initiation of each electrochemical procedure. Low-level aeration was also applied during exposure in order to maintain the required level of aeration or de-oxygenation.

Cold-rolled mild steel (AS/NZS 1595:1998, grade CA1 [14]) and AISI 316 (UNS S31600) stainless steel plate was cut to give dimensions of 1.5 × 25 × 50 mm. Zinc galvanised mild steel coupons were cut from AS 1397, grade Z275 [15] hot-dipped galvanised coil-coated sheet. All metals were mechanically polished and degreased with an acetone/ethanol mixture and completely air dried. Metals were place in contact with the electrolytes immediately after the cleaning sequence.

All measurements were made using a Princeton Applied Research Parstat 2263 potentiostat/galvanostat, which was calibrated according to guidelines published in ASTM G106-89 [16]). Parstat-PowerSuite Version 2.33 software was used in conjunction with ZSimpWin EIS analysis software (Revision 3.00). All data were produced in the potentiostatic mode over a maximum frequency range of 1 mHz to 1 MHz at ± 10 mV of the corrosion potential using a Princeton Applied Research standard flat cell (Model K0235) with an electrolyte volume of approximately 0.5 dm^3 and a working electrode area of 1.0 cm^2. A saturated calomel electrode (SCE) was used in conjunction with a Luggin-Haber capillary and current flowed to and from a high surface area platinum gauze counter electrode. All measurements were performed after an initial, short-term corrosion potential stabilisation period of 2,000 s. The resistances associated with the electrolyte (R_s) and the relative rate of corrosion (R_p) were determined and through equivalent circuit modelling and verified by direct analysis of the spectra, where possible.

Table 2 Specified range of preservative concentrate composition as supplied by each manufacturer

Component	Concentration/% wt./wt.		
	CCA[a]	CuAz[b]	ACQ[c]
Cupric oxide (given as Cu)	12–16 (8.1 ± 1.2)	–	–
Cupric carbonate (given as Cu)	–	12.3 (11.9 ± 0.8)	<10.0 (8.2 ± 1.2)
Chromium trioxide	45–55	–	–
Arsenic pentoxide (given as arsenic acid)	25–35	–	–
Boric acid	–	4.9	–
Tebuncanzole	–	0.5	–
Monoethanolamine		4.6	–
Di-2-ethylhexyl phthalate		<0.2	–
Surfactants and defoamers	–	8.0	–
Didecylthyl ammonium chloride	–	–	<10.0
Free ammonia	–	–	<10.0
Ethanol	–	–	<10.0
Water	Balance	Balance	Balance

Experimentally determined concentrations of copper are given in parenthesis

[a] CCA-C formulation—contains chromium, copper and arsenic as metallic oxides

[b] CA-B formulation—active biocide other than copper is tebuncanzole ($C_{16}H_{22}CN_3O$, molar mass 307.8 g mol^{-1})

[c] ACQ-B formulation—active biocide other than copper is didecylthyl ammonium chloride ($CH_3C_{10}H_{21}NCH_3C_{10}H_{21}Cl$ or DDAC, molar mass 362.1 g mol^{-1})

3 Results and discussion

Nyquist (Cole-Cole or complex impedance plane) plots and equivalent Bode plots were derived for each metal/electrolyte system as a function of exposure time in the electrolyte. In these figures, Z' indicates the real impedance and Z'' is the imaginary component. Frequency is presented as ω and the phase shift as θ. Although presentation of all the plots used for the derivation of the corrosion rate data is beyond the scope of this publication, a complete library of the raw impedance data is available for study from an alternative source [17].

Analysis of the Nyquist and Bode plots showed that within all three of the preservative electrolytes there were at least two discernable time constants for all three of the materials studied. In the simplest case, the resistance value of the time constant at the lower applied frequencies (time constant A) was attributed to the inverse of the rate of the following oxidations:

$$\mathrm{Fe} - 2\mathrm{e}^- \rightarrow \mathrm{Fe}^{2+} \tag{1}$$

$$\mathrm{Zn} - 2\mathrm{e}^- \rightarrow \mathrm{Zn}^{2+} \tag{2}$$

and was generally very large, when compared to time constant B measured at higher frequencies. The reduction of the species in CCA electrolytes under acid conditions have been proposed to involve the cathodic polarisation of the following equilibria [8]:

$$2\mathrm{H_2O} \Leftrightarrow \mathrm{O_2} + 4\mathrm{H^+} + 4\mathrm{e^-} \tag{3}$$

$$\mathrm{H_2} \Leftrightarrow 2\mathrm{H^+} + 2\mathrm{e^-} \tag{4}$$

$$\mathrm{Cu} \Leftrightarrow \mathrm{Cu^{2+}} + 2\mathrm{e^-} \tag{5}$$

$$\mathrm{Cr} + 4\mathrm{H_2O} \Leftrightarrow \mathrm{HCrO_4^{2-}} + 7\mathrm{H^+} + 6\mathrm{e^-} \tag{6}$$

$$\mathrm{As_2O_3} + 5\mathrm{H_2O} \Leftrightarrow 2\mathrm{H_3AsO_4} + 4\mathrm{H^+} + 4\mathrm{e^-} \tag{7}$$

The reduction of copper and oxygen would equally apply to the CuAz and ACQ electrolytes.

Typical examples of Nyquist plots are presented in Figs. 1–4 for mild steel in the diluted CuAz preservative solution, stainless steel in the ACQ solution and the galvanised steel in the CuAz and CCA electrolytes, respectively. From the equivalent Bode plots the intercept of time constant A at $\log_{10} \omega = 0$ in all cases was taken to equal the sum of R_s and R_p. The value of this empirical intercept always increased at variable and highly contrasting rates between systems as a function of exposure time. The corresponding absolute values of Z' at the x-axis intercept of the Nyquist plots, time constant A also varied considerably as a function of the material and electrolyte classification. The value of R_s, however, remained constant for a given electrolyte.

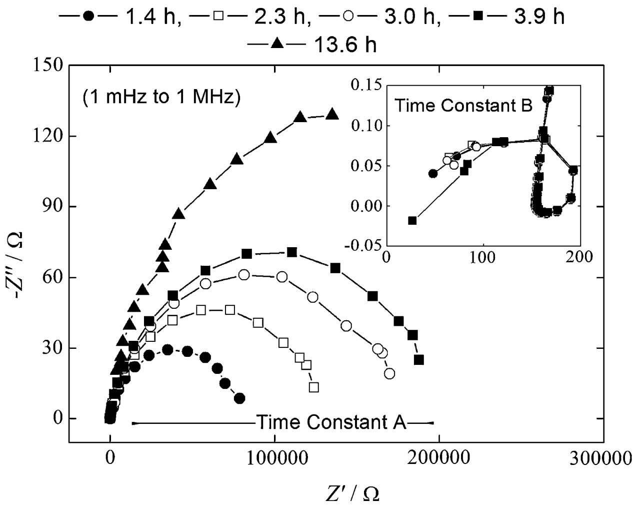

Fig. 1 Nyquist plots for mild steel immersed in a diluted solution (Cu = 0.1 mol dm^{-3}) of CuAz timber preservative as a function of exposure time

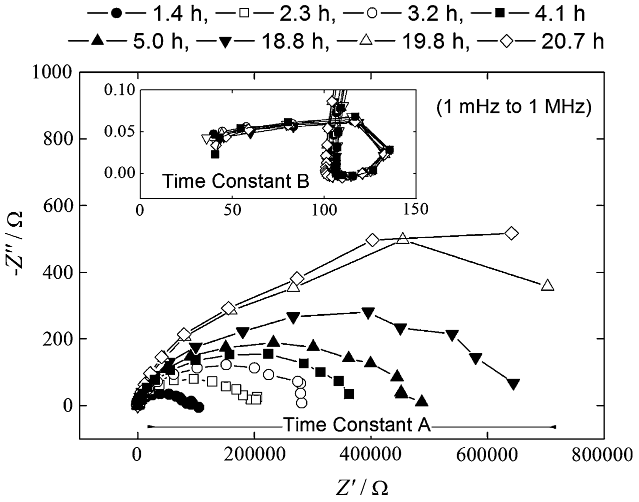

Fig. 2 Nyquist plots for AISI 316 stainless steel immersed in a diluted solution (Cu = 0.1 mol dm^{-3}) of ACQ timber preservative as a function of exposure time

Indeed, the general order of the resistance and capacitance associated with time constant B was generally independent of electrode material and time of exposure and the behaviour was only influenced to any significant extent by the composition/conductivity of the electrolyte. Time constant B is considered to contain a contribution towards the total resistance provided by the electrolyte, i.e., time constant B is a partial component of R_s. The resistance of the electrolyte was never measured solely as a simple R_s value associated with a non-capacitative contribution at the highest applied frequencies. A combination of both non-capacitative and capacitative equivalent circuit elements, therefore, could be used to model the overall response of the aqueous electrolytes. This indicates more complex behaviour than that expected for simple systems, where the electrolyte may be represented by a single resistor in series

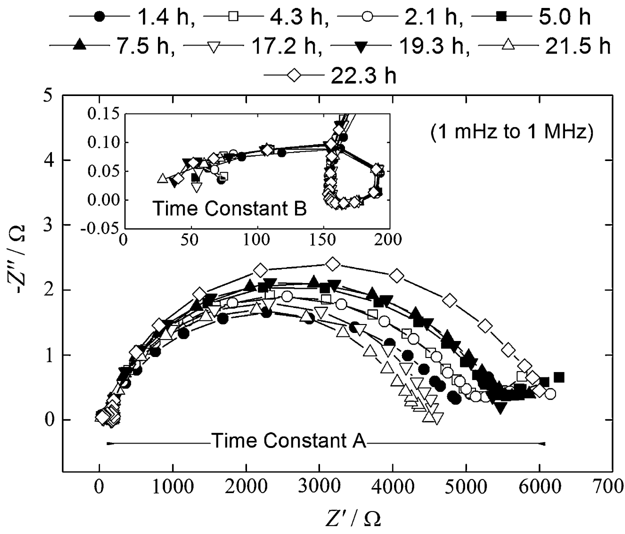

Fig. 3 Nyquist plots for hot-dipped galvanised steel immersed in a diluted solution (Cu = 0.1 mol dm^{-3}) of CuAz timber preservative as a function of exposure time

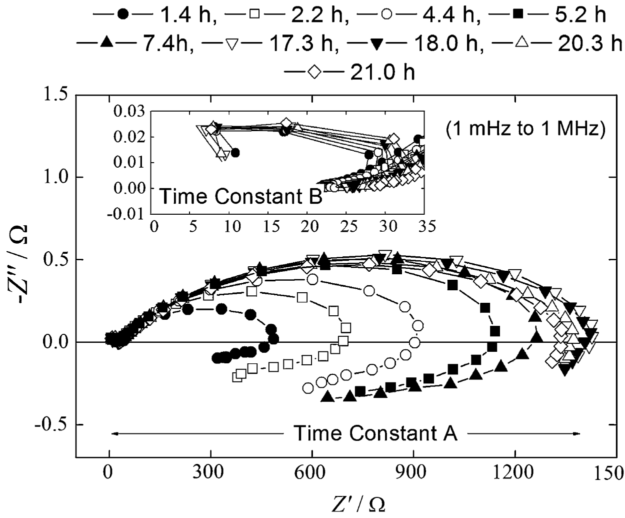

Fig. 4 Nyquist plots for hot-dipped galvanised steel immersed in a diluted solution (Cu = 0.1 mol dm^{-3}) of CCA timber preservative as a function of exposure time

with the circuit elements representing the corrosion process [18–20].

Unlike the time constant B, the resistance and capacitance values of the time constant A varied as a function of working electrode material as noted earlier. These observations describe surface specific behaviour and an increasingly protective quality of the nature of metallic passivation with time of exposure. This reproduces behaviour noted previously with the use of direct current and open circuit electrochemical measurements [9]. It may be assumed, therefore, that the difference in the low and high frequency *x*-axis intercept Z' values associated with the time constant A is directly related to the materials performance through the polarisation resistance of the overall corrosion reaction. Again, the assumed R_p values that can be calculated from this time constant correspond with the previous direct current electrochemistry and the weight loss measurements, i.e., relatively low R_p values, and hence high relative rates of corrosion over time, are associated with the galvanised electrode (Table 1). For the zinc-based material, R_p does not change appreciably with time, thus indicating either (a) a poor capability of protective films when passive, the character of which does not improve significantly with time, or (b) a relatively retarded rate of passivation, the time of which was greater that the period of exposure.

The general response of the Nyquist plots for the mild steel and AISI 316 stainless steel closely resembled those presented in Figs. 1 and 2, regardless of electrolyte type. As will be seen later, this class of EIS response can be modelled accurately using the same equivalent circuit. Values of Z' associated with time constant A of the stainless and mild steels at the low frequency *x*-axis intercept were particularly high (in the order of 0.1 MΩ to 1 MΩ), relative to the galvanised steel (in the range 300 Ω to 10 kΩ). For the galvanised material, therefore, the total resistance associated with time constant A was low and the relative difference in the magnitude of resistance between this constant and time constant B was of lesser significance.

The example given in Fig. 3 for the HDG in the diluted CuAz solution is representative of the responses observed for the hot-dipped galvanised steel in both the CuAz and ACQ timber preservative solutions. With reference to Fig. 1, which incorporates the same electrolyte, note also the identical behaviour of time constant B with that given in Fig. 3. This behaviour is typical as, throughout this work, it was noted that the nature of this time constant was identical for a given electrolyte, regardless of electrode material used.

The hot-dipped galvanised steel in the CCA electrolyte (Fig. 4) produced a distinct EIS response compared to all the other systems. The extent of the time constant B for this system, in terms of the value of Z' assumed to be associated with R_s, is of a lower order than that measured for either the CuAz or the ACQ electrolytes (refer to Figs. 1–3). This is due to the factor of seven-times higher conductivity of the diluted CCA electrolyte relative to the equivalent CuAz electrolyte. It is indicated that a reduced net ionic migration under polarisation within the CuAz electrolyte has resulted in a measurable increase in ohmic drop associated with the solution resistance. This effect was also replicated in the ACQ electrolytes which have poor ionic conductivity relative to the CCA.

Each EIS response was modelled against the library of equivalent circuits contained within the ZimpWin software (see, for example, Figs. 5–7). Each equivalent circuit

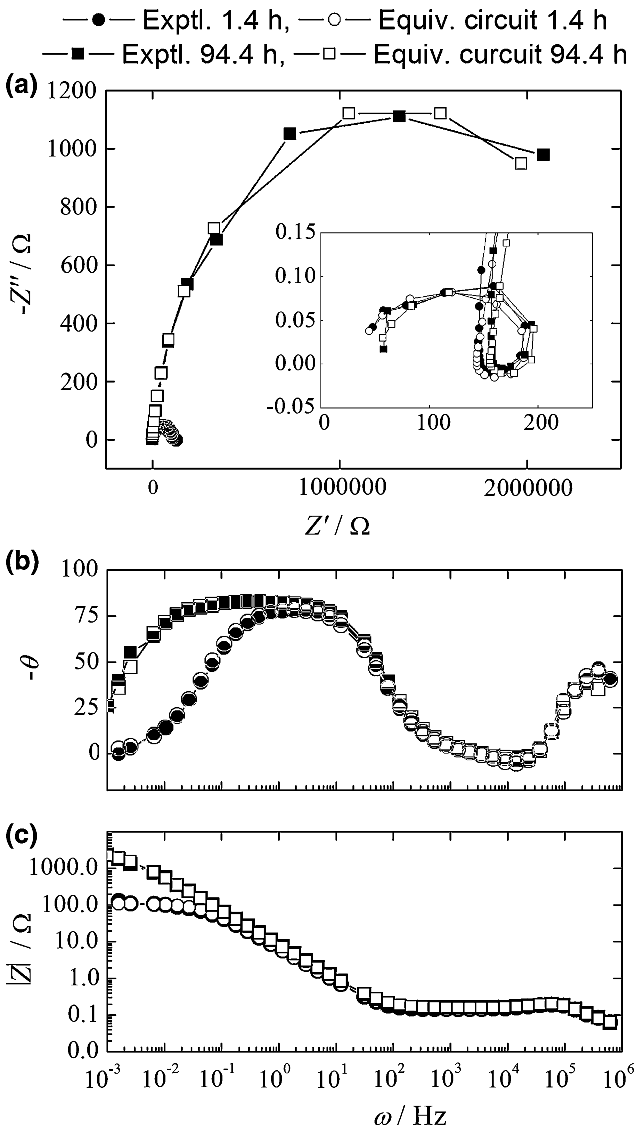

Fig. 5 AISI 316 stainless steel in the diluted CuAz electrolyte. (**a**) Nyquist and (**b**) and (**c**) Bode responses that are typical of the behaviour of the mild steel and stainless steel in all electrolytes when Equivalent Circuit I ($R1(C1R2(L1R3))(Q1R4)$) is applied. The notation, 'exptl' and 'equiv. circuit' indicate empirical and modelled data, respectively

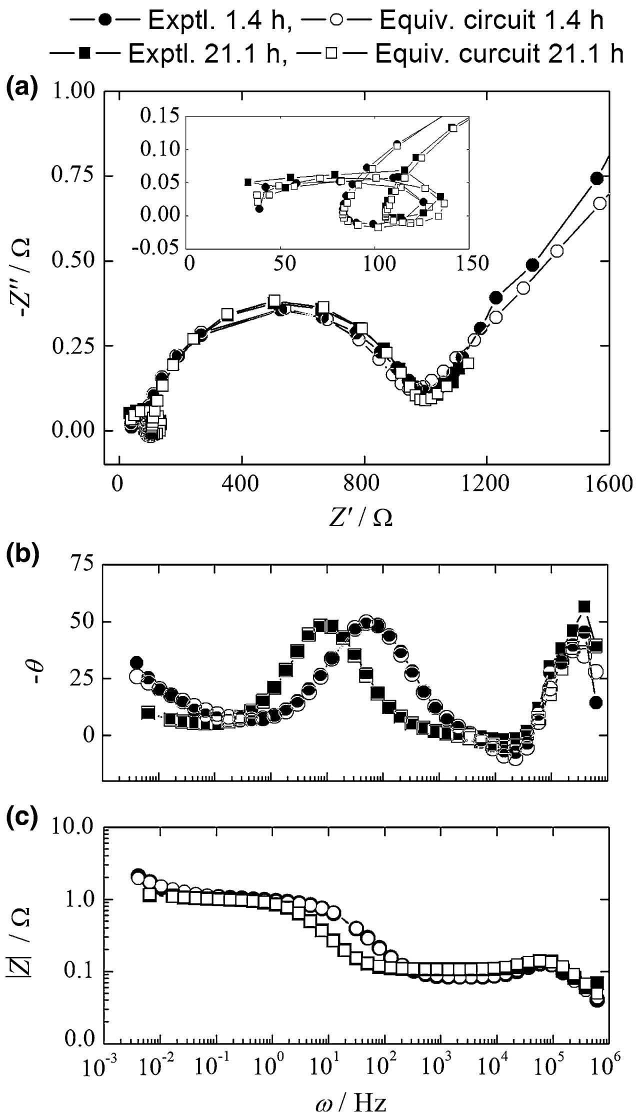

Fig. 6 The hot-dipped galvanised steel in the CuAz electrolyte. (**a**) Nyquist and (**b**) and (**c**) Bode responses that are typical of the behaviour of the galvanised steel in the CuAz and the ACQ electrolytes when the Equivalent Circuit II ($R1(C1R2(L1R2))(Q1(R4W1))$ is applied. The notation, 'exptl' and 'equiv. circuit' indicate empirical and modelled data, respectively

provided a reasonable correlation with the experimental data and, when applicable, produced final R_s and R_p values which were always strictly equivalent to those that could be estimated directly.

The small, initial non-capacitance influenced resistance at the highest frequencies was universally termed $R1$ (Fig. 8a). For every system examined in this work, time constant B consistently appeared to be most ideally modelled by the notation $C1R2(L1R3)$. See also Fig. 8b, where $R2$ and $R3$ are resistance elements and $C1$ is a capacitance element. The additional 'looping' observed on all the Nyquist plots immediately after the low frequency end of the time constant B can be modelled as an inductive behaviour by considering element $L1$ [21].

The most acceptable fit to the time constant A responses at the lower applied frequencies could be modelled using one of the three circuit classifications given in Fig. 9. Equivalent Circuit I (Fig. 9a) was a simple electronic model that was able to reproduce the behaviour of mild steel and 316 stainless steel in all of the 0.1 mol dm^{-3} Cu aqueous timber treatments. Q relates to constant phase element and, as Fig. 9 shows, this circuit component has been included as a non-ideal capacitor equivalent. Values of Q are considered as an empirical constant and have been applied to simulate the characteristically compressed

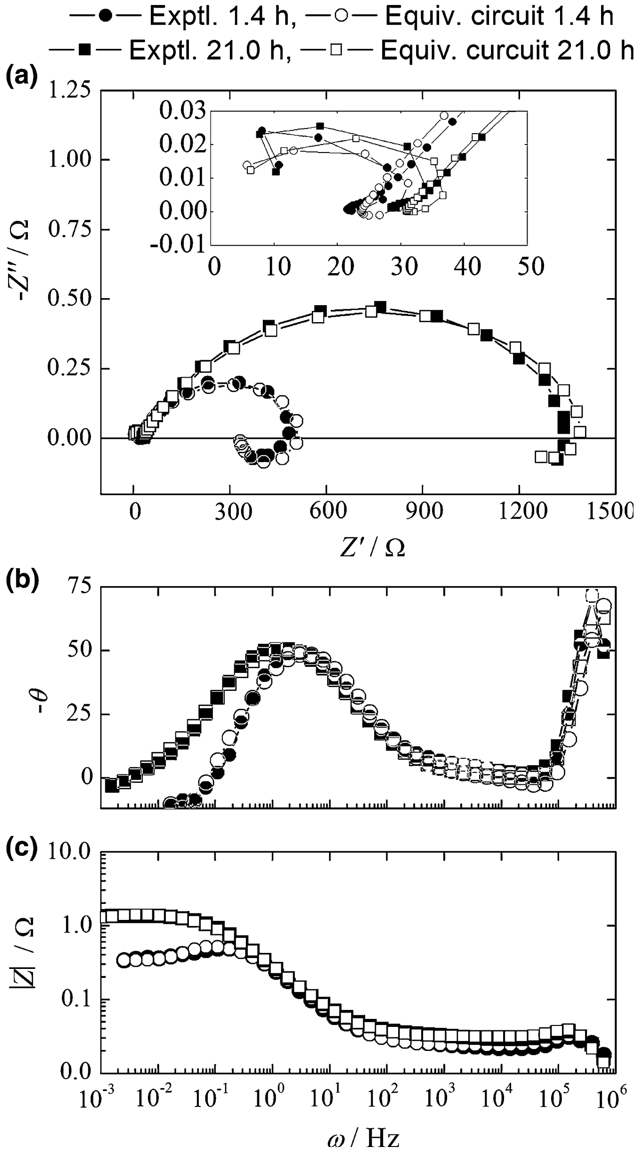

Fig. 7 The hot-dipped galvanised steel in the CCA electrolyte. (**a**) Nyquist and (**b**) and (**c**) Bode responses are typical of the behaviour of the galvanised steel in the CCA electrolyte when Equivalent Circuit III ($R1(C1R2(L1R3))(Q1R4(L2R5))$) is applied. The notation, 'exptl' and 'equiv. circuit' indicate empirical and modelled data, respectively

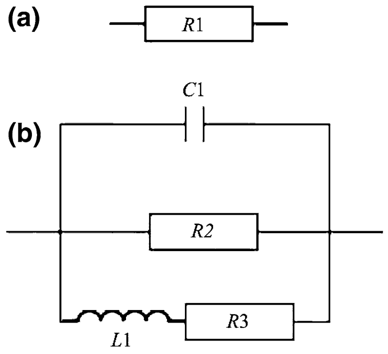

Fig. 8 Equivalent circuits used to model the EIS response of (**a**) $R1$ and (**b**) time constant B. The notation, 'exptl' and 'equiv. circuit' indicate empirical and modelled data, respectively

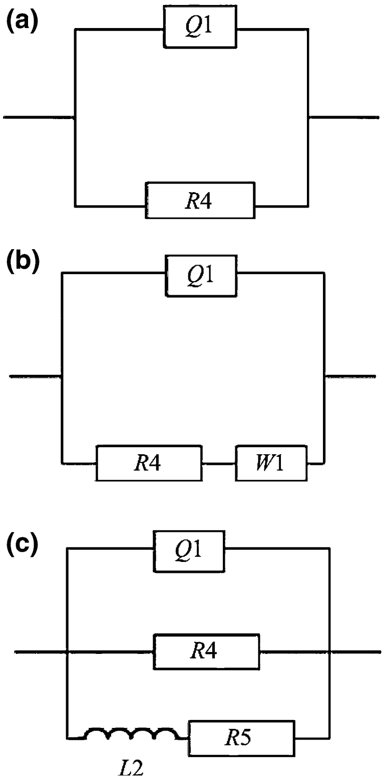

Fig. 9 Electronic circuits used to model the EIS response of time constant A. (**a**) Equivalent Circuit I (**b**) Equivalent Circuit II and (**c**) Equivalent Circuit III

nature of the 'semi-circular' time constant A when viewed via a Nyquist plot. Warburg impedance (W) has been incorporated within Equivalent Circuit II (Fig. 9b) to model the low frequency response that was usually observed for the hot-dipped galvanised steel in the diluted ACQ and CuAz aqueous timber preservatives (see Fig. 6). Thus, a diffusion controlled processes has been simulated, such as species transfer through surface films or mass transport through the electrolyte. Equivalent Circuit Type III (Fig. 9c) was used to represent the hot-dipped galvanised steel in the diluted CCA aqueous timber preservative. Inductance is included in this equivalent circuit as analogous inductive behaviour was also observed at the low frequency end of time constant A for this particular system (Fig. 4).

For each electrolyte, the mean values of the resistance elements $R1$, $R2$ and $R3$ were calculated from the EIS responses of each electrochemical system as a function of time. Note that all of the $R1$ values, when calculated within a electrolyte type as a function of working electrode material, were generally identical. The short term exposure values of $R1$ in the CCA electrolyte were less than 10 Ω for all three materials. Higher values are indicated for the CuAz and ACQ media (20 to 60 Ω). Mean $R2$ and $R3$ values measured for the diluted CCA solution ranged from approximately 30 to 80 Ω and 30 to 83 Ω, respectively. The CuAz electrolyte, with the lowest conductivity of 0.0048 S cm^{-1}, consistently gave the highest $R2$ and $R3$ resistance values of all the electrolytes with $R2$: 145 to 205 Ω and $R3$: 180 to 420 Ω. The clear distinction between electrolytes in terms these R values was independent of working electrode type and further supports the inference that $R1$, $R2$ and $R3$ were all associated with electrolyte resistance and not the rate of corrosion. R_s was calculated for each system using:

$$R_s = R1 + \frac{1}{(1/R2 + 1/R3)}. \tag{8}$$

R_s was independent of electrode materials and constant over the times of immersion studied in this work. The calculated values of R_s were 24 ± 2 Ω (CCA), 100 ± 2 Ω (ACQ) and 149 ± 4 Ω (CuAz). The magnitude and relative order of these values closely replicate the directly measured ionic resistivity of the electrolytes, the latter of which can be calculated from the ionic conductivities given in the introductory section.

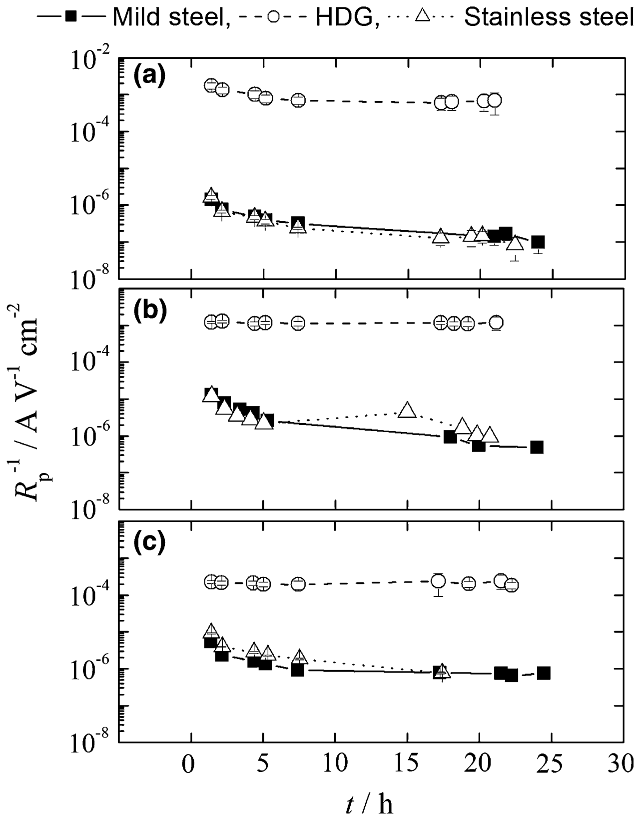

Fig. 10 Mean values of EIS derived relative rates of corrosion as calculated for the mild steel, hot-dipped galvanised steel and 316 stainless steel corrosion rates in the diluted (**a**) CCA (**b**) ACQ and (**c**) CuAz electrolytes. The time axis is common to all three plots

Assuming that the inverse polarisation resistance for each of the corrosion reactions was related to the total resistance associated with time constant A, relative rates of corrosion were derived as a function of material and electrolyte type (Fig. 10). The hot-dipped galvanised steel repeatedly produced the highest overall values of inverse polarisation resistance, which were of the order 10^{-4} A V^{-1} cm^{-2} for the CuAz and 10^{-3} A V^{-1} cm^{-2} for the ACQ and the CCA) electrolytes. Such values were two or four orders of magnitude greater than either the mild steel or the stainless steel (10^{-7} to 10^{-6} A V^{-1} cm^{-2}). The relative rates of metallic dissolution of the hot-dipped galvanised steel strongly indicate active behaviour the zinc under the conditions of the test. Conversely, the extremely low values of inverse polarisation resistance determined for the ferrous materials indicate effective materials passivation as previous noted using the weight loss and direct current analyses (see Table 1).

These results also substantiate conclusions derived from a thermodynamic study which examined the influence of pH and galvanic interactions of the metallic ions in aqueous CCA, CuAz and ACQ preservatives [8]. It was predicted that solid zinc corrosion products/passivating layers would not be stable at either low or high solution pH. In comparison to iron, there are also particularly large negative Gibbs free energy changes (ΔG) associated with the zinc oxidation (reaction [2]). This is facilitated by the Cu^{2+}, present in all the diluted electrolytes ($\Delta G_{\text{reaction}}$ −225 kJ mol^{-1}), and species such as $HCrO_4^-$, H_3AsO_4 present in the CCA formulation ($\Delta G_{\text{reaction}}$ −672 and −502 kJ mol^{-1} at pH 2 or −640 and −320 kJ mol^{-1} at pH 10, respectively).

4 Conclusions

4.1 The impedance responses of the ferrous- and zinc-based materials in the CCA, CuAz and ACQ electrolytes indicate that an analogous capacitance influence is associated with both the corrosion mechanism and with the solution resistance of each of the electrolytes.

4.2 The spectra have been modelled using a simple equivalent circuit analysis, from which, the resistance polarisation associated with each of the corrosion reactions has been extracted.

4.3 The extracted relative rates of corrosion follow general trends in data taken from previous short-term weight loss and direct current methodologies taken in similar electrolytes, where, for short-term exposure periods, it has been concluded that

(a) hot-dipped galvanised steel will corrode in an active manner at rates that can be orders of magnitude greater than that of mild steel and 316 stainless steel and

(b) the ferrous-based materials corrosion rates suggest effective passivation in most instances.

4.4 These results contrast with those taken from solid timber electrolytes [7]. It is clear that aqueous timber preservative electrolytes should not be used in a simple manner to predict the corrosion rate of mild steel or hot-dipped galvanised materials in preservative treated wood.

Acknowledgements This work was performed in the laboratories of BRANZ Ltd. (New Zealand) and funded by the New Zealand Building Research Levy. Concentrations of aqueous copper in the preservative concentrates were determined by Spectrachem Analytical Ltd. (New Zealand).

References

1. Anon (2005) Arsenic Technical Report, The reconsideration of registrations of arsenic timber treatment products (CCA and arsenic trioxide) and their associated labels, Australian Pesticides And Veterinary Medicines Authority, Canberra, Australia
2. Anon (2003) Commission Directive 2003/2/EC, Relating to restrictions on the marketing and use of arsenic (tenth adaptation to technical progress to Council Directive 76/769/EEC), Scientific Committee on Toxicity, Ecotoxicity and the Environment, Brussels, Belgium
3. Anon (2003) Federal Register: FR09AP03-58, Response to requests to cancel certain chromated copper arsenate (CCA) wood preservative products and amendments to terminate certain uses of other CCA products, United States Environmental Protection Agency, Washington, USA
4. NZS 3640 (2003) Chemical preservation of round and sawn timber, Standards New Zealand, Wellington, New Zealand
5. Lebow S (2004) Research Paper FPL-RP-618, Alternatives to chromated copper arsenate for residential construction. United States Department of Agriculture, Forest Service, Forest Products Laboratory, Madison, USA
6. Anon (2004) PR-1, Techline: changes in pressure-treated wood for residential construction, Forest Products Laboratory, United States Department of Agriculture, Madison, USA
7. Kear G, Wú H-Z, Bruce EW, Kane C, Jones MS (2007) Corros Mater 32:16
8. Kear G, Wú H-Z, Jones MS (In press—DOI 10.1617/s11527-007-9338-6) Mater Struct
9. Kear G, Wú H-Z, Walsh FC (In press) Aust J Chem doi: 10.1071/CH07429
10. Anon (2004) T-PTW00D04 1/04 exp. 1/05, Technical Bulletin: preservative treated wood, Simpson Strong-Tie Company, Inc., Dublin, USA
11. AWPA E17 (1999) Standard method for determining corrosion rates of metals in contact with treating solution, American Wood-Preservers' Association, Alabama, USA
12. Stern M, Geary AL (1957) J Electrochem Soc 104:56
13. Wojtowicz M, Piwowarczyk W (2002) Ochrona Przed Koroja 12:328 (Polish)
14. AS/NZS 1595 (1998) Cold-rolled, unalloyed, steel sheet and strip, Standards Australia/Standards New Zealand, Homebush, Australia/Wellington, New Zealand
15. AS 1397 (1993) Steel sheet and strip-hot-dipped zinc-coated or aluminium/zinc coated, Standards Australia, Homebush, Australia
16. ASTM G 106 (1989) Standard practice for verification of algorithm and equipment for electrochemical impedance measurements, ASTM International, West Conshohocken, USA
17. Kear G, Wú H-Z (2006) SR153, The corrosion of metallic fastener materials in untreated, CCA-, CuAz-, and ACQ-based timbers. BRANZ, Judgeford, New Zealand
18. MacDonald DD (1977) Transient techniques in electrochemistry. Plenum Press, London, UK
19. Lorenz WJ, Mansfeld F (1981) Corros Sci 21:647
20. MacDonald JR, Johnson WB (1987) In: Macdonald JR (ed) Impedance spectroscopy: emphasizing solid materials and systems, Wiley, New York, USA, pp 1–26
21. Raistrick ID, Franceschetti DR, MacDonald JR (2005) In: Barsoukov E, Macdonald RJ (eds) Impedance spectroscopy: theory, experiment, and applications, Wiley, New Jersey, USA, pp 27–75